Title: **Domains of the hepatitis B virus small surface protein S mediating oligomerization**

Running title: HBV S oligomerization

Authors: Sascha Suffner[1], Nadine Gerstenberg[1], Maria Patra[1], Paula Ruibal[1,2], Ahmed Orabi[1,3], Michael Schindler[1,4] and Volker Bruss[1#]

Institutions: [1]Institute of Virology, Helmholtz Zentrum München, Ingolstädter Landstraße 1, D-85764 Neuherberg, Germany
[2]Present address: Department of Infectious Diseases, Leiden University Medical Center, Leiden, The Netherlands
[3]Department of Virology, Faculty of Veterinary Medicine, Zagazig University, Sharkia Governorate, Egypt
[4]Institute for Medical Virology, University Hospital Tübingen, Tübingen, Germany.

[#]Corresponding author: Volker Bruss
Institute of Virology
Helmholtz Zentrum München
Ingolstädter Landstraße 1
D-85764 Neuherberg
Germany
Phone: x49 89 3187 3021
Fax: x49 89 3187 3329
email: volker.bruss@helmholtz-muenchen.de

Key words: Hepatitis B virus, membrane protein, protein oligomerization

Words count in abstract: 247

Words count in text: (excluding ref., tables, Fig. legends) 6857

Abstract

During hepatitis B virus infections subviral particles (SVP) consisting only of viral envelope proteins and lipids are secreted. Heterologous expression of the small envelope protein S in mammalian cells is sufficient for SVP generation. S is synthesized as a transmembrane protein with N-terminal (TM1), central (TM2), and C-terminal (HCR) transmembrane domains. The loops between TM1 and TM2 (CL) and between TM2 and HCR (LL) are located in the cytosol and in the ER lumen, respectively. To define domains of S mediating oligomerization during SVP morphogenesis S mutants were characterized by expression in transiently transfected cells. Substitution of 12 out of 15 amino acids of TM1 to alanines as well as the deletion of HCR still allowed SVP formation demonstrating that these two domains were not essential for contacts between S proteins. Furthermore, the oligomerization of S was measured with a FACS-based FRET (Foerster resonance energy transfer) assay. This approach demonstrated that CL, TM2, and LL independently contributed to S oligomerization while TM1 and HCR played a minor role. Apparently, intermolecular homooligomerization of CL, TM2, and LL drive S protein aggregation. Detailed analyses revealed that the point mutation C65S in CL, the exchange of 13 out of 19 amino acids of TM2 to alanine residues, and the simultaneous substitution of all eight cysteine residues in LL by serine residues blocked the ability of these domains to support S protein interactions. Altogether, specific domains and residues were defined in the HBV S protein required for oligomerization and SVP generation.

Importance

The small hepatitis B virus envelope protein S has the intrinsic capability to direct the morphogenesis of spherical 20 nm subviral lipoprotein particles. Such particles expressed in yeast or mammalian cells represent the antigenic component of current hepatitis B vaccines. Our knowledge about the steps leading from the initial, monomeric, transmembrane translation product of S to SVP is very limited as is our information on the structure of the complex main epitope of SVP that induces the formation of protective antibodies after vaccination. This study contributes to our understanding of the oligomerization process of S chains during SVP formation and shows that the cytoplasmic, one membrane embedded, and the luminal domain of S independently drive S-S oligomerization.

Introduction

The hepatitis B virus (HBV) is the prototype member of the virus family *hepadnaviridae* and causes chronic hepatitis in a substantial fraction of infected humans (1) (2). The virus particle consists of an icosahedral capsid with a diameter of 30 nm containing a partially double stranded circular DNA genome and an outer lipid envelope carrying three surface proteins: the large envelope protein L, the middle-sized M protein, and the small S protein (3). During infection of the human liver virions are secreted from the hepatocytes into the blood stream and in addition subviral particles (SVP) in up to 10^4-fold excess over virions. These SVP appear as spheres or filaments with a diameter of 20 nm consisting solely of lipid and viral envelope proteins (4) (5). Both, the envelope of virions and SVP express the same antigenicity (hepatitis B surface antigen, HBsAg). Clearance of the virus and immunity depend on the formation of antibodies against HBsAg.

Heterologous expression of S in eukaryotic cells causes the secretion of spherical SVP consisting of lipid and approximately 100 copies of the S protein (6). Expression of S in yeast does not lead to SVP secretion. However, lipoprotein complexes of S can be purified from yeast cells (7) and represent the major active hepatitis B vaccine. The structure of the S protein in yeast derived particles is partially different from the structure in SVP secreted by mammalian cells (8). E.g. approximately half of S is N-glycosylated at asparagine 146 in S derived from infected patients or transfected eukaryotic cells but S from yeast carries no glycan residue. Additionally, disulfide bridges are different between mammalian and yeast derived S. A detailed structure of S in SVP is still missing. Crystallization of SVP was unsuccessful up to now, although a relatively low resolution image has been obtained with cryo-EM (9).

The pathway leading from newly translated S protein to secreted SVP is only partially characterized. The S protein is cotranslationally inserted into the ER membrane. This insertion is first initialized by an N-terminal type I signal [containing transmembrane domain 1 (TM1), aa 8 to 22] which directs the N terminus of S into the ER lumen and is not cleaved off (Fig. 1). A central type II translocation signal (containing TM2, aa 80 to 98) initiates a second transmembrane translocation, in this case of the peptide chain C-terminal of TM2, and anchors the protein in the ER membrane in a N terminus cytoplasmic - C terminus ER luminal orientation (10, 11). The combination of signal I and II generates a cytosolic loop (CL) between TM1 and TM2 and a luminal loop (LL) downstream of TM2. Asparagine 146 in LL is partially cotranslationally N-glycosylated. A proposed amphipathic helix (aa 156 to 169) may be attached to the inner leaflet of the ER membrane. The location of the hydrophobic C-terminal region (HCR, aa 170 to 226) relative to the membrane is less clear. Since the region between aa 196 and 201 is critical for the envelopment of the cytoplasmic hepatitis D virus nucleoprotein (12) it is conceivable that this part faces the cytoplasm whereas the C terminus of S is oriented towards the ER lumen (10). This suggests that two more transmembrane areas exist between aa 170 and 226.

Shortly after synthesis the S protein forms disulfide bridged dimers (13). The N-glycosylation has no influence on dimer formation. Models for the folding of S based on theoretical assumptions have been published (14), however, the number and positions of intra- and intermolecular disulfide bridges in S dimers are not known. Correct disulfide bridges are fundamental for the formation of the main epitope of HBsAg (15).

For SVP formation S dimers float horizontally in the cellular membrane and must oligomerize to higher complexes thereby substantially excluding host proteins since

only HBV envelope proteins have been detected in SVP (5). However, intermediate oligomers have not been observed to date. Particle formation probably takes place at a membrane of the secretory pathway between ER and Golgi complex (16). This step may not resemble the process of virion budding and may represent a totally different mechanism (17). While virion budding depends on cellular factors involved in the budding of vesicles from multivesicular bodies, SVP formation does not. During subsequent passage of the luminal SVP by vesicular transport through the Golgi apparatus the N-linked glycans are modified from the mannose rich type to the complex type. Finally, SVP are further transported via vesicles towards the cell membrane and released from the cell.

Intracellular S is mainly dimeric and carries almost exclusively mannose rich glycans whereas secreted SVP carry predominantly complex glycans. This suggests that the period of time between dimerization of S in the ER membrane and sugar modification in the Golgi complex is rather large (hours) compared to the period of time between protein translation and dimerization (minutes) as well as to the time span between sugar modification and release (minutes). Possibly, the step leading from transmembrane S to luminal SVP is the time-consuming process.

We intended to define the pathway of SVP formation in more detail and performed a comprehensive study clarifying the contribution of S domains to S oligomerization. The experimental approach was based on coexpression of S proteins or parts of S linked to the fluorescent proteins YFP and BFP in transiently transfected cells. Proximity between a YFP- and BFP-linked construct could be measured by Foerster resonance energy transfer (FRET).

Materials and Methods

Plasmids. The plasmid pSVBX24H carries the PstI (nt 21) to the BglII (nt 1982) fragment of an HBV genotype A genome (18) and directs the expression of the wild type HBV S gene (nt 153 to 830) under control of an simian virus 40 early promoter. For easier detection of the S protein on western blots a DNA stretch coding for the hemagglutinin derived epitope YPYDVPDYA (HA) was inserted between the last codon of the S gene and its stop codon generating the S variant H. By site directed in vitro mutagenesis the 8 cysteine codons at positions 107, 121, 124, 137, 138, 139, 147, and 149 of the H gene were mutated to serine codons generating variant H*. In H the codons 10 to 20 were changed to alanine codons causing the mutation of TM1 from FLGPLLVLQAGFFLL to $FLA_{11}LL$ and generating variant H.1pA. In H the codons 83 to 95 were changed to alanine codons causing the mutation of TM2 from RRFIIFLFILLLCLIFLLVLLD to $RRFIIA_{13}VLLD$ and generating variant H.2pA. In H.12pA both poly-alanine substitutions in TM1 and TM2 were combined. For the construction of H.Δ178 and H.Δ153 codon 178 or 153, respectively, was mutated in the H background into a stop codon.

For the construction of Y-TM2 a DNA sequence encoding R78 to D99 (TM2) of the S protein followed by the 9 codons for the HA epitope and a stop codon was fused 3' to the YFP open reading frame in plasmid peYFP-N1 (19) with a $(GA)_3$ linker sequence in between (…BsrG1 site -> TGTACA AG GGA GCA GGT GCA GGA GCA CGG <- R78 of S). For B-TM2 the same TM2-HA coding sequence was fused to the XhoI site of plasmid pmTagBFP-C1 (20) (XhoI site -> CTCGAG CT CGG <- R78 of S). For Y-HTR a DNA sequence coding for the type II signal CSGSICYGTIAVIVFFLIGFMIGYLGY from the human transferrin receptor (21) fused to the HA coding sequence was ligated 3' to the YFP open reading frame of plasmid

peYFP-N1 (linker: BsrG1 site -> TGTACA AG GGA GCA GGA GCA TGT <- N-terminal cysteine codon of transmembrane domain of HTR). For B-HTR the HTR-HA sequence was fused 3' to the BFP open reading frame in plasmid pmTagBFP-C1 (linker: XhoI site -> CTCGAG CT TGT <- N-terminal cysteine codon of transmembrane domain of HTR). B/Y-MEM was constructed by fusing the N-terminal 20 amino acids of neuromodulin (22) to the N terminus of YFP and BFP using plasmids peYFP-N1 and pmTagBFP-C1, respectively. The neuromodulin fragment contains a signal for posttranslational palmitoylation of cysteines 3 and 4 that targets the fusion proteins to cellular membranes.

The construction of the expression plasmid for the fusion protein between the fluorescent protein mCherry carrying an N-terminal secretion signal and the HBV S protein (construct C-S) which is competent for subviral particle secretion is described elsewhere (23). For the construction of Y-S and B-S the mCherry derived part in C-S was substituted by open reading frames coding for YFP or BFP, respectively. #B-S and #Y-S were constructed by digesting the plasmids for the expression of Y-S and B-S with BamHI uniquely cutting in the region encoding the N-terminal signal sequence and with XmaI cutting downstream of the HBV derived insertion. The corresponding fragment was inserted into BamHI-XmaI digested pSVBX24H. Using Y/B-S the cysteine codons 107, 121, 124, 137, 138, 139, 147, and 149 of the S gene were mutated to serine codons resulting in constructs Y/B-S*. The derivatives Y/B-S*.1pA, Y/B-S*.2pA, Y/B-S*.12pA, Y/B-S*.Δ178, and Y/B-S*.Δ153 were constructed in the same way as the corresponding H variants (see above). For Y/B-S. Δ100 a stop codon was introduced at codon 100 of Y/B-S*. For Y/B-S*.C65S the cysteine codon 65 in the S open reading frame in Y/B-S* was changed into a serine codon. In Y/B-S.12pAΔ100, Y/B-S.C65S-12pAΔ100, Y/B-S*.C65S-2pA the corresponding

mutations were combined. Y/B-S.C65S-2pA corresponds to Y/B-S*.C65S-2pA but the codons 107, 121, 124, 137, 138, 139, 147, and 149 of the S gene code for cysteines like in the wild type.

Cell culture, transfection, harvest. Huh7 cells grown in 12-well dishes were transiently transfected with a total amount of 0.5 µg of plasmid using Fugene HD (Promega), or X-tremeGene (Roche) according to the instructions of the manufacturer. In case of cotransfections an equal molar ratio of plasmids was used. After transfection the culture supernatant was removed, the cells were washed twice with 1 ml of PBS, and 1 ml of fresh medium was added to the cells. Five days post transfection the culture supernatant was harvested and centrifuged for 10 minutes at 13.000 rpm. From the supernatant 40 µl were used for western blotting. The cells on the dish were washed with 1 ml of PBS and lysed by adding 0.25 ml of lysis buffer [50 mM Tris-HCl pH 7.5, 100 mM NaCl, 20 mM ethylendiamintetraacetate, 0.5 % (v/v) Nonidet P40] and incubation on ice for 10 minutes. The cell lysate was collected and spun at 13,000 rpm for 10 minutes. Ten µl of the supernatant were used for western blotting.

Cell fractionation. Cells transiently transfected in 6-well dishes were washed 3 days post transfection twice with 1 ml of ice-cold PBS and incubated 45 minutes with 0.4 ml of 10 mM Tris-Cl, pH 7.4, 150 mM NaCl, 1 % (v/v) Triton X-114 on ice (24). The cell lysate was collected and spun for 45 minutes at 12,000 g and 4°C. Ten µl of the supernatant was used for western blotting (total lysate). From the supernatant 350 µl was layered on top of 350 µl of a cushion of 6**%** (w/v) sucrose, 10 mM Tris-HCl, pH 7.4, 150 mM NaCl, 0.06% (v/v) Triton X-114 and incubated for 5 minutes at 30°C. After centrifugation for 3 minutes at 12,000 g and RT, 20 µl of the upper phase was used for western blotting (aqueous phase). The remaining part of the aqueous phase

was removed. Twenty µl of the detergent phase was used for western blotting (membrane fraction).

Western blotting. Cleared cell culture supernatants or lysates of transfected Huh7 cells were denatured and reduced with sodium dodecylsulfate and dithiothreitol and used for electrophoresis through 12 % polyacrylamide gels. The proteins in the gel were transferred onto nitrocellulose membranes (Amersham Protran 0.45 NC, GE Healthcare) by wet blotting. Proteins were detected with a rabbit antibody against the HA epitope (Sigma-Aldrich Chemie GmbH, Schnelldorf, Germany) for all constructs carrying this tag and with a cross-reacting rabbit anti-GFP (D5.1XP, New England Biolabs, Ipswich, USA) antibody in case of YFP fusion proteins. As a loading control western blots were stained with rabbit anti-β-tubulin (New England Biolabs, Ipswich, USA). The HBV S protein was detected with the monoclonal anti-HBs antibody HB1 (courtesy provided by Aurelia Zvirbliene, Vilnius University, Lithuania). Rabbit antibodies against calnexin and PDI were from New England Biolabs Ipswich, USA. Peroxidase-labeled antibodies against rabbit and mouse immunoglobulins were from Dianova (Hamburg, Germany).

FACS-FRET. The FRET analysis was done as described by Banning and colleagues (19). One day after transfection in 12-well dishes Huh7 cells were washed twice with PBS, detached from the dish with 100 µl of trypsin solution and suspended in 800 µl of 1 % (v/v) FCS in PBS. Cells were then sedimented by centrifugation at 1,300 rpm and 4°C for 5 minutes and the cell pellet was suspended in 200 µl of 1 % (v/v) FCS in PBS and applied to the FACS machine. BFP was excited with a laser beam of 405 nm wavelength, its emission was measured at 450 nm. YFP was excited with laser light of 488 nm wavelength and its emission was measured at 529 nm.

Rate zonal sedimentation. A sucrose gradient consisting of 0.5 ml of 60 % (w/w) sucrose in 50 mM Tris-HCl, pH 7.4, 100 mM NaCl, 0.1 mM EDTA, and 1 ml each of corresponding 45 %, 35 %, 25 %, and 15 % sucrose solutions was prepared in centrifugation tubes and left for 4 hours at 4°C. Then 0.5 ml of culture supernatant was layered on top, and the gradient spun for 16 hours at 50,000 rpm and 10°C in a Beckman SW55 rotor. The gradient was harvested from the top (15 x 0.33 ml fractions). The sucrose concentration of the fractions was measured by refractometry and the distribution of proteins was analyzed by western blotting using the monoclonal anti-HBs antibody HB1.

Protease protection experiment. The preparation of microsomes and the protease protection experiments were done as described elsewhere (25) with the exception that cells have not been labeled with radioactive methionine and the samples were not used for immunoprecipitation prior to polyacrylamide gel electrophoresis. Instead, 10 µl of each sample were denatured and loaded directly onto the gel.

Immunofluorescence. Cells were seeded on cover slips and transfected the next day. Two days post transfection cells were washed twice with PBS and fixed by incubation with 4 % paraformaldehyde for 15 minutes at room temperature. Cells were washed again three times for 5 minutes each with PBS and shaking and incubated with ice cold methanol for 10 minutes at -20°C. After washing again with PBS cells were incubated for 1 hour in 5 % (v/v) goat serum, 0.3 % (v/v) Triton X-100 in PBS. Cells were then incubated with a rabbit anti-PDI antibody (New England Biolabs) diluted 1:200 in 1 % (w/v) bovine serum albumin, 0.3 % (v/v) Triton X-100 in PBS (antibody dilution buffer) or with the monoclonal anti-HBs antibody HB1 diluted 1:100 in the same buffer overnight at room temperature in a humid box. After washing three times for 5 minutes with PBS and shaking cells were incubated with

an Alexa 555 labeled goat anti-rabbit antibody (Life Technologies) diluted 1:2,000 in antibody dilution buffer or with an Alexa 488 labeled goat anti-mouse antibody (Life Technologies) diluted 1:2,000 in the same buffer for 2 hours at room temperature in the dark. After washing three times with PBS for 5 minutes each cells were fixed with MOWIOL (Sigma-Aldrich) and stored at 4°C until examined with a fluorescence microscope.

Results

Experimental strategy. During the oligomerization phase the three topologically separated parts of S (cytosolic, transmembrane, and luminal part) can directly interact only with parts of other S chains being in the same compartment. Therefore, we could simplify the question “Which parts of S mediate oligomerization?” to “Do cytosolic (transmembrane, luminal) domains of S interact with cytosolic (transmembrane, luminal) domains of other S chains during oligomerization?”

Transmembrane domains. We started with the membrane compartment of S consisting of transmembrane domains TM1, TM2, and HCR and asked whether interactions between these domains could be measured and whether such interactions are required for SVP formation. Former work suggested that TM2 might be important (26). Because TM2 is part of an autonomous type II translocation/anchor signal it was possible to assay TM2 separately from other parts of S for its ability to interact with other TM2 domains.

Heterologous expression of TM2. TM2 and three flanking charged amino acids (aa) in the S protein chain (sequence: RRFIIFLFILLLCLIFLLVLLD) were fused to the

C terminus of the fluorescent proteins YFP and BFP, respectively, and a short hemagglutinin epitope (HA) tag was added at the C terminus of TM2 (Fig. 2A) in the background of a SV40 early promoter expression vector (B-TM2 and Y-TM2). As controls, similar chimeras with a substitution of the central 13 aa of TM2 with a poly-alanine stretch (sequence: RRFIIA$_{13}$VLLD, constructs B-2pA and Y-2pA) and with an exchange of TM2 by the type 2 signal sequence of the human transferrin receptor (B-HTR and Y-HTR) were generated. The resulting six chimeras were expected to form transmembrane proteins carrying the fluorescent moiety at the cytoplasmic side of the membrane (Fig. 2B). All six constructs could easily be detected by anti-HA antibodies on western blots of cell lysates after transient transfection of Huh7 cells with the corresponding plasmids (Fig. 2C). After fractionation of these cells into a soluble and membranous part all three YFP-fused proteins were only found in the membrane fraction (Fig. 2D) like the ER transmembrane protein calnexin and not in the soluble fraction like the ER luminal enzyme protein disulfide isomerase (PDI) suggesting that TM2 and its derivative 2pA as well as the HTR derived signal were functional.

Oligomerization of Y-TM2 with B-TM2 via the TM2 domain was measured by FRET between their fluorescent moieties in living cells (Fig. 2E, Fig. 2F) using FACS analyses (FACS-FRET) (19). To detect FRET signals by flow cytometry, we used a rigorous gating strategy that finally gives the fraction of BFP positive cells showing a FRET signal. In detail, we define a FRET gate (gate P3) by measuring the background signal using cells that were transfected to coexpress untagged BFP and YFP only (Fig. 2F, panel Y+B). The FRET gate is set in a way that less than 0.5 % of these cells exert FRET. As a positive control, we utilized cells transfected to express a BFP-YFP fusion protein, which were expected to yield close to 100 % FRET positive cells (panel Y-B). The results of the measurements were expressed as the

percentage of cells shifting into the FRET gate, which was set according to the negative and positive controls. Approximately 30 % of Y-TM2 plus B-TM2 coexpressing cells showed a positive FRET signal (Fig. 2E, lane 7, Fig. 2F, panel Y/B-TM2) indicating proximity of the two proteins. Coexpression of Y-TM2 (Fig. 2E, lane 3) or B-TM2 (lane 4) with non-membrane anchored BFP or YFP as a negative control generated no FRET signal. As an additional negative control, we used derivatives of YFP and BFP carrying the 20 N-terminal aa from neuromodulin (Y/B-MEM) at their N termini (22). This short aa stretch contains a signal for post-translational palmitoylation of cysteine residues and causes membrane attachment of the proteins. Coexpression of Y-TM2 (lane 5) or B-TM2 (lane 6) with a B-MEM or Y-MEM, respectively, resulted in no significant FRET indicating that measured FRET signals were not induced by overexpression or unspecific interactions at cellular membranes.

The positive FRET signal of Y-HTR/B-HTR coexpressing cells indicated that the transmembrane domain of HTR mediated oligomerization between both proteins (Fig. 2E, lane 9, Fig. 2F, panel Y/B-HTR). Moreover, coexpression of the TM2 and HTR constructs (Fig. 1E, lanes 10 and 11) resulted in very low or no significant FRET signals. This showed that the interaction between TM2 domains was not simply the result of general hydrophobic interactions between transmembrane domains but depended on specific protein-protein contacts. Coexpression of Y-2pA and B-2pA generated no FRET signal (Fig. 2E, lane 8, Fig. 2F, panel Y/B-2pA) and demonstrated that the central 13 aa of TM2 were important for the interaction.

Requirements of transmembrane domains for SVP formation.

TM2. We tested the importance of TM2-TM2 interactions in the background of a wild type (WT) S protein carrying an HA tag at the C terminus (construct H, Fig. 3A).

Changing the central 13 aa of TM2 to alanine residues (mutant H.2pA) allowed efficient expression (Fig. 3B, upper panel, lane 3) but blocked the appearance of SVP in the culture supernatant (lower panel). This indicates that the poly-alanine mutation in TM2 which still supported its function as a translocation and anchor signal (Fig. 2D) but blocked TM2-TM2 interactions (Fig. 2E) also inhibited later steps in SVP formation.

TM1. The type I translocation signal TM1 could not be evaluated in analogy to TM2 (Fig. 2) because it has no membrane anchor function and would only result in translocation of a fused peptide chain across the ER membrane (27) (at a C-terminal position TM1 would not be functional at all). Therefore, TM1 (sequence: FLGPLLVLQAGFFLL) was tested in the background construct H by changing the central 11 aa to alanine residues (mutant H.1pA; TM1 sequence $FLA_{11}LL$, Fig. 3A). This rather drastic change was compatible with the release of the mutant into the culture supernatant with slightly reduced efficiency relative to construct H (Fig. 3B, lower panel, compare lanes 1 and 4) and with SVP formation as suggested by rate zonal sedimentation in sucrose gradients (Fig. 3C). This indicates that a potential specific interaction of TM1 with transmembrane sequences of S were probably not essential for SVP morphogenesis.

HCR. A C-terminal deletion of H (H.Δ178, Fig. 3A) eliminating aa 178 to 226 of S removes the putative third and fourth transmembrane domains but keeps the assumed amphipathic helix. This mutant was released from transfected cells (Fig. 3B, lane 6) as SVP (Fig. 3C) indicating that the HCR downstream of aa 177 was not required for particle formation. Particles formed by this mutant sedimented slightly slower relative to SVP consisting of H (or S, see Fig. 4A) since the peak was shifted two fractions to the top and are possibly smaller than 20 nm. Further deletion of the

amphipathic helix (construct H.Δ153) blocked the appearance of SVP in the culture supernatant (lane 7). The expected molecular weight of unglycosylated H.Δ178 was approximately 20 kDa which fits to the apparent molecular weight observed in western blots. However, H.Δ153 showed an apparent molecular weight of approximately 22 kDa, while the expected value was 17 kDa. We cannot explain this effect.

In summary, only TM2-TM2 interactions seem to be crucial for SVP formation in the membrane compartment whereas HCR could be deleted and TM1 could be changed drastically without blocking SVP formation.

Investigating the contribution of individual parts of S to oligomerization in the background of fluorescent S fusion proteins.

To measure the influence of mutations in S on oligomerization by FRET we intended to construct fusion proteins of YFP and BFP with S. The phenotype of these chimera should resemble the phenotype of WT-S as close as possible. Prior studies showed that a C-terminal fusion of GFP to S did not result in a construct capable of efficient SVP formation (28). Moreover, the N-terminal fusion to S allowed only very inefficient SVP formation (28). However, the fusion of such a large domain to the N terminus of S is expected to cause the inhibition of the first membrane translocation of the S part (TM1 is nonfunctional at an internal position in a peptide chain). By adding an N-terminal secretion signal to an mCherry-S fusion (23) (Fig. 4A, upper panel) we intended to correct the transmembrane topology of the chimera which should then have the same topology as the middle-sized HBV envelope protein M. In the M protein the translocation signal TM1 is able to direct the translocation of the 55 aa long N-terminal preS2 domain into the ER lumen because this domain is relatively short (27). By this approach we were indeed able to generate a fluorescent S

derivative which was secreted into the culture supernatant as efficiently as WT S protein (middle panel). Rate zonal sedimentation showed that the chimera formed subviral particles (lower panel). These particles sedimented slightly faster than 20 nm particles which is consistent with their expected larger size.

The mCherry construct, however, was not used in our FRET experiments because the energy transfer between mCherry and YFP or BFP would be inappropriate. Therefore, we fused the type I secretion signal from the enzyme β-lactamase to the N terminus of YFP-S and BFP-S, respectively (constructs Y-S and B-S, Fig. 4B). For unknown reasons, the Y-S and B-S constructs did not form detectable amounts of subviral particles (data not shown). However, the transmembrane topology of the Y-S and B-S chimera appeared as expected confirmed by protease protection experiments (Fig. 4C). When microsomes were prepared from cells expressing these constructs by douncing and sedimentation the YFP and BFP moieties were not digested by trypsin (lanes 5 and 11) unless the membranes were opened by the addition of detergent (lanes 6 and 12). This phenotype indicates translocation of the protected domains into the ER lumen and was similar to the behavior of the preS2 domain of the M protein (lanes 2, 3). When the secretion signal sequence was missing at the N terminus (construct #B-S), the BFP moiety was also digested in the absence of detergent as expected (lane 14). The larger apparent molecular weight of B-S relative to #B-S is caused by covalent modifications of the BFP moiety like N-glycosylation occurring in the ER lumen (29). This supports the notion that the topology of B-S is similar to the M protein These result motivated us to use the Y-S and B-S constructs for FRET analyses to define domains of S involved in S oligomerization.

Mutation of luminal cysteine residues to serine residues. LL contains 8 of the 14 cysteine residues of the S protein. This domain very efficiently mediated oligomerization (probably dimerization) of S (see below) which is stabilized very early after translation by intramolecular disulfide bridges between S chains (13). By changing all 8 cysteine residues in LL to serine residues LL loses its property to support oligomerization (see below). In fact, the resulting construct in the H background (H*, the star indicates the substitution of all luminal cysteine residues in all constructs) did not form disulfide linked oligomers as evident after gel electrophoresis under non-reducing conditions (data not shown), and H* was not able to generate secreted SVP although its expression level was only slightly reduced in comparison to H (Fig. 3B, lanes 1 and 2). We introduced the 8 serine to cysteine mutations in LL of the Y-S and B-S constructs resulting in Y-S* and B-S* (Fig. 4B), respectively, in order to be able to measure the influence of mutations in other parts of S on oligomerization by FRET. Expression levels of the Y/B-S* derivatives were slightly lower relative to Y/B-S (Fig. 4D), however, the FRET signals were comparable (Fig. 4F). All further mutants based on constructs Y/B-S (Fig. 4B) could be detected in transiently transfected Huh7 cells, although their expression levels were slightly different (Fig. 4D, E). All constructs carrying the N-glycosylation site of the S moiety at N146 appeared as double bands on western blots most probably due to partial N-glycosylation at this site (Fig. 4D). All constructs missing N146 showed a single band (Fig. 4E). Mutant Y-S*.Δ153 (Fig. 4D, lane 7, labeled with a star) generated two double bands: one at the expected position corresponding to approximately 55 kDa molecular weight and an unexpected one at approximately 70 kDa. The Δ153 C-terminal truncation of construct H also showed an abnormal molecular weight after gel electrophoresis (Fig. 3B, lane 7). We have no explanation for this observation so far.

Furthermore, we compared the intracellular distribution of the Y-S fusion and several selected mutants with the WT S protein by immunofluorescence (Fig. 4G). The S protein was detected using a polyclonal anti-HBs antibody and a fluorescent secondary antibody, while the other constructs were visualized by their fluorescence. In addition the ER was labeled with an antibody against the ER resident protein protein disulfide isomerase (PDI), and the Golgi complex was stained by cotransfection of an expression vector for a fluorescent galactosyltransferase I (30). All proteins showed a diffuse staining of the ER and a more punctuated pattern in the Golgi complex like the WT S protein.

Transmembrane domains. Substitution of the central 13 aa of TM2 with alanine residues which blocked TM2-TM2 interactions in the Y/B-TM2 background (constructs Y/B-2pA, Fig. 2) reduced the FRET signal in the Y/B-S* background only from 97 % to 78 % (compare Fig. 4F, lanes 4 and 5). This indicates that other elements than TM2 contributed to S protein interactions. TM1 was also tested in the context of Y/B-S* by the poly-alanine substitution of the central 11 aa (construct Y/B-S*.1pA, Fig. 4B). This change reduced the FRET signal from 97 % to 60 % (Fig. 4F, lane 6) suggesting that TM1 supports the formation or stabilization of S oligomers. The combined alanine substitutions in both TM1 and TM2 (Y/B-S*.12pA) showed a positive FRET signal of 68 % (Fig. 4F, lane 7). The differences between the 1pA, 2pA, and 12pA derivatives were statistically not significant.

Removing HCR by introduction of the Δ178 truncation into the Y/B-S* background (constructs Y/B-S*.Δ178) resulted in a marked decrease of FRET signals to 42 % (Fig. 4F, lane 8). Apparently, HCR also supports S oligomerization. The additional removal of the putative amphipathic helix in construct Y/B-S*.Δ153 reduced the

FRET signal to 35 % (lane 9). The difference of the FRET signal between Y/B-S*.Δ178 and Y/B-S*.Δ153 was not statistically significant.

Cytosolic loop. To investigate whether the CL between TM1 and TM2 mediates contacts between S chains during oligomerization we introduced the point mutation C65S into this region in the Y/B-S* background (mutants Y/B-S*.C65S, Fig. 4B). It is not expected that cysteine 65 is part of a disulfide bridge because the redox state of the cytosol generally prevents cystine formation in this compartment. Prior studies demonstrated that the C65S point mutation completely blocked SVP secretion (31). The C65S mutation also strongly reduced the FRET signal from 97% to 22% when introduced into the Y/B-S* pair (Fig. 4F, lane 13). Although a profound effect of the conservative point mutation on the gross folding of the S protein cannot be fully excluded it seems rather unlikely. A more plausible explanation is that the mutation blocked interactions of S chains via CL or interactions of this loop with unknown cellular factors supporting the oligomerization of S chains.

In the mutant Y/B-S.12pA Δ100 the transmembrane domains TM1 and TM2 are mutated by poly-alanine stretches and LL as well as HCR are deleted. Therefore, the only remaining part of the S protein is CL. This construct still showed a low but measurable FRET signal (Fig. 4F, lane 14) suggesting homodimer formation by intermolecular interactions of CL domains. The introduction of the C65S point mutation in CL in this background (constructs Y/B-S.C65S-12pA Δ100), however, completely abolished the FRET signal (lane 15) supporting this notion. The background threshold of the assay (dashed line in Fig. 4F) was defined as the average of at least three negative control transfections (unfused BFP + YFP) plus three times their standard deviation.

Luminal loop. The mutant Y/B-S.Δ100 lacks not only HCR and the putative amphipathic helix but in addition LL. This construct showed a FRET signal of 42% (Fig. 4F, lane 10) which is comparable to the FRET signal of Y/B-S*.Δ153 (Fig. 4D, lane 9) carrying in addition LL with the cysteine to serine mutations. This result suggests that LL with the eight cysteine to serine point mutations did not contribute to the oligomerization of S chains.

In Y/B-S*.C65S-2pA we combined the 2pA mutation (substitution of the central 13 aa of TM2 by alanine residues) blocking TM2-TM2 interactions with the C65S mutation in CL and the cysteine to serine mutations in LL. This mutant generated no detectable FRET signal (Fig. 4F, lane 12). This strengthens the statement that TM1 and HCR were not sufficient to establish measurable contacts between S chains. Restoring all 8 cysteine residues of LL of this mutant (resulting in Y/B-S.C65S-2pA) restored the FRET signal to WT (97%, Fig. 4F, lane 11) indicating that LL was able to efficiently mediate S oligomerization independent of functional CL and TM2 when expressed in the context of full length S protein.

Altogether, our results showed that TM1 and HCR were not essential for S interactions whereas LL, TM2, as well as CL independently mediated S oligomerization. In addition, we describe mutations blocking the homooligomerization of these three domains.

Discussion

During SVP morphogenesis approximately 100 transmembrane HBV S proteins assemble with lipids forming a spherical lipoprotein particle of 20 nm diameter. Since host proteins are efficiently excluded during S protein aggregation and SVP

morphogenesis it has to be assumed that specific interactions between the assembling proteins are required for this process. The present study aimed to identify regions in S which were crucial for S protein interactions during this process.

On the one hand, this study was simplified by the fact that the topologically separated areas of S could directly interact only with areas of other S chains in the same compartment (CL with CL; LL with LL; TM1, TM2, and HCR with each other). On the other hand, the study was relatively complex because it turned out that three areas of the S protein (CL, TM2, and LL) independently mediated S-S interactions. We were finally able to define the contribution of each domain by FACS-FRET analysis because we could generate an S mutant carrying relatively subtle mutations in CL (C65S), TM2 (a poly-alanine stretch), and LL (point mutation of all 8 cysteine residues to serine residues) that showed no FRET signal anymore (Y/B-S*.C65S-2pA, Fig. 4D). This mutant could be used as a background to individually reintroduce the WT version of CL (Y/B-S*.2pA), TM2 (Y/B-S*.C65S), and LL (Y/B-S.C65S-2pA). All three variants exhibited strong or medium FRET signals (Fig. 4F, lanes 5, 13, 11) suggesting that each one of CL, TM2, and LL was sufficient for generating measurable protein interactions.

The most direct evidence for a specific contribution to S-S interactions was obtained for TM2 (Fig. 2) since this element could be tested isolated from other parts of S due to the autonomous functionality of the type 2 translocation signal. Prior studies (26) also suggested a role of TM2 in this process since the exchange of TM2 in S by the type 2 translocation signal of the human transferrin receptor with identical length or by TM2 from the duck hepatitis B virus S protein resulted in a stable chimera that was unable (i) to form SVP, (ii) to form mixed particles with WT S, and (iii) to inhibit SVP formation by coexpressed WT S. This phenotype indicated that the chimera und

WT S did not form stable, mixed oligomers. Apparently, the changes in TM2 prevented a stable interaction. Also in the background of a full-length S protein fused to YFP and BFP the protein contacts were mediated by TM2 (compare Y/B-S*.C65S with Y/B-S*.C65S-2pA, see previous paragraph). A contribution of transmembrane domains to the assembly of viral envelope proteins has also been reported for other viruses (32).

TM1 seems to be less important for stable S oligomer formation than TM2. Indeed, the exchange of 11 aa by alanine residues reduced FRET signals from 97 % to 60 % (Fig. 4F, lane 4 and 6), however, this mutation was compatible with SVP formation in the H background (Fig. 3B, lane 4 and Fig. 3C). Furthermore, the replacement of TM1 by the type 1 secretion signal from β-lactamase allowed SVP secretion in the background of the middle-sized HBV envelope protein M carrying additional 55 aa (preS2 domain) at the N terminus of S (26). The large HBV envelope protein L [carrying additional 119 aa (preS1 domain) at the N terminus of M] generates two different transmembrane topologies: one with a cytoplasmic preS1 domain (i-preS) and the other with a luminal preS1 domain (e-preS) (25, 33, 34). It is expected that TM1 in the S domain of L chains with an i-preS conformation is not traversing the membrane, but is located like preS1, preS2, and LL on the cytoplasmic side of the ER membrane. The i-preS form of L is, however, incorporated into the envelope of virions and into SVP. This supports the model that TM1 as a transmembrane domain is not required for HBV envelope protein assembly.

The HCR was clearly not required for S protein oligomerization since its deletion allowed SVP formation (H.Δ178, Fig. 3B, lane 6 and Fig. 3C). Nevertheless, the deletion caused a reduction of protein-protein interactions as measured by FRET (Fig. 4F, lane 8). Apparently, this interaction was not essential for SVP formation. A

similar C-terminal deletion of the S protein at position L176 (35) resulted in a stable protein not forming SVP which was, however, incorporated into SVP when coexpressed with WT S protein. In this S mutant a few foreign aa residues were fused C-terminally to L176 due to the cloning strategy which may cause the phenotypic difference to H.Δ178. The formation of mixed particles, however, also indicates that HCR was not essential for a stable interaction of S protein chains.

The authentic sequence of TM1 and the presence of HCR were not necessary for SVP formation and therefore not for S protein assembly. Both domains were also not sufficient for S protein dimerization since the constructs Y/B-S*.C65S-2pA containing WT TM1 and HCR generated no FRET signal (Fig. 4F, lane 12). This phenotype underlines the minor role of TM1 and HCR in S protein oligomerization.

The domain LL had the strongest effect on oligomerization. Changing the 8 cysteine to serine mutations in LL of mutant Y/B-S*.C65S-2pA to WT restored the FACS signal from negative to the WT level (Fig. 4F, compare lane 12 and 11). This might also be explained by the fact, that LL-LL interactions are stabilized by disulfide bridges covalently locking the interaction partners.

A positive FRET signal indicates proximity of coexpressed YFP/BFP pairs. However, it does *per se* not distinguish whether the proximity is created early in the SVP morphogenesis pathway (like dimer formation) or later (like higher oligomer formation). It is, however, very likely that dimerization is a prerequisite for the formation of higher complexes. Therefore, we propose that the three domains CL, TM2, and LL are involved in dimer formation (Fig. 5). The proposed model does not explain how S dimers form higher oligomers and exclude host protein during assembly. A conceivable possibility is that the proposed amphipathic helix (aa 156 – 169) or C-terminal parts of the luminal loop mediate contacts between S dimers and

therefore support the generation of higher oligomers. Alternative approaches will be needed to clarify the requirements for the formation of higher multimers.

Acknowledgments

This work was funded by institutional support to V.B. from the Helmholtz Zentrum München. A.O. was supported by the Deutscher Akademischer Austauschdienst (DAAD) in cooperation with the Egyptian Ministry of Higher Education and Scientific Research.

Figure Legends

FIG. 1. Model for the transmembrane topology of the HBV S protein monomer in the ER membrane (large grey bar). TM1, TM2: transmembrane domains 1 and 2, CL: cytosolic loop, LL: luminal loop, HCR: hydrophobic C-terminal region. Small box: putative amphipathic helix, (G): facultative glycan N-linked to N146, C65: cysteine residue at position 65. Numbers refer to aa positions. Domains located in the ER lumen (cytosol) are located on the surface (in the inside) of secreted SVP.

FIG. 2. TM2-TM2 interactions. (A) Map of constructs consisting of an N-terminal YFP or BFP moiety fused to TM2, a derivative of TM2 with alanine substitutions of the central 13 aa (2pA), or the type II signal of the human transferrin receptor (HTR). An influenza virus hemagglutinin tag (HA) was fused to the C terminus. (B) Expected transmembrane topology of the constructs. (C) Western blot from lysates of cells expressing the six constructs stained with anti-HA (upper panel) or anti-tubulin (lower

panel) as a loading control. (D) Western blot of cells transfected with the indicated YFP constructs and separated into soluble (s) and membrane (m) fractions, (t): unfractionated total cell lysate. Staining was performed with antibodies (ab) against the HA tag of the fusion proteins, against calnexin as an ER luminal and soluble protein, against PDI as an ER transmembrane protein, and against tubulin as a cytosolic soluble protein (ab). The YFP constructs appeared exclusively in the membrane fraction. Numbers and bars at the left: position of molecular weight markers. (E) FACS-FRET analysis. Cells cotransfected with the indicated YFP (Y) / BFP (B) pairs were used for FACS-FRET analysis. MEM: palmitoylated 20 aa domain causing membrane attachment of the fusion protein. Y-B: YFB-BFP fusion protein. The ordinate indicates the fraction of BFP-positive cells showing a positive FRET signal. Dashed line: background threshold. TM2 domains specifically interacted with each other. (F) FACS plot of cells (co-) transfected with the indicated constructs. The gate P3 excluded cells with background FRET signals.

FIG. 3. Influence of mutations in transmembrane domains of S on SVP formation. (A) Map of S derivatives. Black boxes: transmembrane domains, gray box: putative amphipathic helix, hatched box: HA tag. C->S: point mutations of all 8 cysteine residues in LL to serine residues. 1pA (2pA): substitution of the central 11 (13) aa of TM1 (TM2) by alanine residues. Δ178, Δ153: C-terminal deletions. The number indicates the position of the stop codon. (B) Western blots of cell lysates (upper two panels) and culture supernatants (lower two panels) stained with the indicated antibodies (ab). Numbers and bars at the left: position of molecular weight markers. The 1pA mutation and the Δ178 truncation were compatible with secretion. (C) SVP formation by secretion competent mutants. Culture supernatants of cells expressing the indicated constructs were sedimented through a sucrose gradient. Proteins were

detected in gradient fractions by western blotting using an HA antibody (upper panels, numbers at the left indicate the position of molecular weight markers), and sucrose concentration (w/w) of the fractions were measured (lower panels).

Fig. 4. Influence of mutations in S on oligomerization. (A) A fluorescent derivative of S competent for SVP formation. Upper panel: Map of the fusion protein C-S carrying an N-terminal secretion signal (sig). Middle panel: Western blot of lysates and culture supernatants of cell expressing WT S or C-S stained with a monoclonal anti-HBs antibody. Lower Panel: Western blot of fractions from a sucrose gradient after rate zonal centrifugation. (B) Map of constructs. All constructs carry a YFP or BFP moiety (hatched box) at the N terminus preceded by a secretion signal (small black box). TM1, TM2, HCR: transmembrane domains and hydrophobic C-terminal region; grey box: putative amphipathic helix; pA: substitution of the central 11 (in case of TM1) or 13 (in case of TM2) aa by alanine residues, C->S: substitution of all 8 cysteine residues in LL by serine residues; C65S: exchange of cysteine 65 by serine. Numbers at the right refer to the lanes in panel F. (C) Transmembrane topology of Y-S and B-S chimera. Microsomes from cells expressing the indicated proteins were treated with trypsin in the absence or presence of mild detergent. The S protein was resistant against trypsin cleavage. The preS2 domain of the M protein was only cleaved when microsomes were opened (lane 3) as expected (25). B-S showed a phenotype equivalent to M, Y-S was not efficiently cleaved. #Y-S and #B-S are similar to Y-S and B-S, respectively, but lack the N-terminal secretion signal. (D and E) Western blots of lysates from cells expressing the indicated constructs. Upper panels: staining with anti-GFP (cross-reacting with YFP), lower panels: staining with anti-tubulin as a loading control. Panel in (E) was developed 5 times longer than panels in (D). Numbers and bars at the left: position of molecular weight markers. (F)

FACS-FRET signals from cells expressing the indicated YFP/BFP pairs. Y + B: coexpression of YFP and BFP, Y-B: fused YFP-BFP chimera. Dashed line: background threshold. (G) Intracellular distribution of Y-S derivatives. Cells expressing the indicated constructs (autofluorescence, green) and a fluorescent version of the Golgi enzyme GalT (GalT-CFP, blue) were stained with an antibody against the ER resident protein PDI (red) and analyzed by immunofluorescence. The WT S protein was stained with polyclonal anti-HBs and a second fluorescent antibody. The bars indicate a distance of 12 µm. All constructs show a diffuse pattern in the ER and a punctuated pattern in the Golgi complex like the WT S protein.

Fig. 5. Proposed model for the S homodimer. The TM2 domains of two S proteins interact with each other as well as the two CL and the two LL domains. Homodimerization of LL is stabilized by intermolecular disulfide bridges (-S-S-). The authentic sequence of TM1 and the presence of HCR were not required for SVP formation. Small circular area: cysteine 65. N: N terminus.

References

1. **Lavanchy D.** 2004. Hepatitis B virus epidemiology, disease burden, treatment, and current and emerging prevention and control measures. J Viral Hepat **11:**97-107.
2. **Seeger C, Mason WS.** 2015. Molecular biology of hepatitis B virus infection. Virology **479-480:**672-686.
3. **Bruss V.** 2007. Hepatitis B virus morphogenesis. World J Gastroenterol **13:**65-73.
4. **Ganem D, Varmus HE.** 1987. The molecular biology of the hepatitis B viruses. Annu Rev Biochem **56:**651-693.
5. **Heermann KH, Goldmann U, Schwartz W, Seyffarth T, Baumgarten H, Gerlich WH.** 1984. Large surface proteins of hepatitis B virus containing the pre-s sequence. J Virol **52:**396-402.

6. **Laub O, Rall LB, Truett M, Shaul Y, Standring DN, Valenzuela P, Rutter WJ.** 1983. Synthesis of hepatitis B surface antigen in mammalian cells: expression of the entire gene and the coding region. J Virol **48:**271-280.
7. **Valenzuela P, Medina A, Rutter WJ, Ammerer G, Hall BD.** 1982. Synthesis and assembly of hepatitis B virus surface antigen particles in yeast. Nature **298:**347-350.
8. **Diminsky D, Schirmbeck R, Reimann J, Barenholz Y.** 1997. Comparison between hepatitis B surface antigen (HBsAg) particles derived from mammalian cells (CHO) and yeast cells (Hansenula polymorpha): composition, structure and immunogenicity. Vaccine **15:**637-647.
9. **Gilbert RJ, Beales L, Blond D, Simon MN, Lin BY, Chisari FV, Stuart DI, Rowlands DJ.** 2005. Hepatitis B small surface antigen particles are octahedral. Proc Natl Acad Sci U S A **102:**14783-14788.
10. **Eble BE, Lingappa VR, Ganem D.** 1986. Hepatitis B surface antigen: an unusual secreted protein initially synthesized as a transmembrane polypeptide. Mol Cell Biol **6:**1454-1463.
11. **Eble BE, MacRae DR, Lingappa VR, Ganem D.** 1987. Multiple topogenic sequences determine the transmembrane orientation of the hepatitis B surface antigen. Mol Cell Biol **7:**3591-3601.
12. **Komla-Soukha I, Sureau C.** 2006. A tryptophan-rich motif in the carboxyl terminus of the small envelope protein of hepatitis B virus is central to the assembly of hepatitis delta virus particles. J Virol **80:**4648-4655.
13. **Wunderlich G, Bruss V.** 1996. Characterization of early hepatitis B virus surface protein oligomers. Arch Virol **141:**1191-1205.
14. **Berting A, Hahnen J, Kroger M, Gerlich WH.** 1995. Computer-aided studies on the spatial structure of the small hepatitis B surface protein. Intervirology **38:**8-15.
15. **Mangold CM, Unckell F, Werr M, Streeck RE.** 1995. Secretion and antigenicity of hepatitis B virus small envelope proteins lacking cysteines in the major antigenic region. Virology **211:**535-543.
16. **Huovila AP, Eder AM, Fuller SD.** 1992. Hepatitis B surface antigen assembles in a post-ER, pre-Golgi compartment. J Cell Biol **118:**1305-1320.
17. **Prange R.** 2012. Host factors involved in hepatitis B virus maturation, assembly, and egress. Med Microbiol Immunol **201:**449-461.
18. **Valenzuela P, Quiroga M, Zaldivar J, Gray R, Rutter W.** 1980. The nucleotide sequence of the hepatitis B viral genome and the identification of the major viral genes. UCLA Symp Mol Cell Biol **18:**57-70.
19. **Banning C, Votteler J, Hoffmann D, Koppensteiner H, Warmer M, Reimer R, Kirchhoff F, Schubert U, Hauber J, Schindler M.** 2010. A flow cytometry-based FRET assay to identify and analyse protein-protein interactions in living cells. PLoS One **5:**e9344.
20. **Subach OM, Gundorov IS, Yoshimura M, Subach FV, Zhang J, Gruenwald D, Souslova EA, Chudakov DM, Verkhusha VV.** 2008. Conversion of red fluorescent protein into a bright blue probe. Chem Biol **15:**1116-1124.
21. **McClelland A, Kuhn LC, Ruddle FH.** 1984. The human transferrin receptor gene: genomic organization, and the complete primary structure of the receptor deduced from a cDNA sequence. Cell **39:**267-274.
22. **Skene JH, Virag I.** 1989. Posttranslational membrane attachment and dynamic fatty acylation of a neuronal growth cone protein, GAP-43. J Cell Biol **108:**613-624.

23. **Bayer K, Banning C, Bruss V, Wiltzer-Bach L, Schindler M.** 2016. Hepatitis C Virus Is Released via a Noncanonical Secretory Route. J Virol **90:**10558-10573.
24. **Bordier C.** 1981. Phase separation of integral membrane proteins in Triton X-114 solution. J Biol Chem **256:**1604-1607.
25. **Bruss V, Lu X, Thomssen R, Gerlich WH.** 1994. Post-translational alterations in transmembrane topology of the hepatitis B virus large envelope protein. EMBO J **13:**2273-2279.
26. **Siegler VD, Bruss V.** 2013. Role of transmembrane domains of hepatitis B virus small surface proteins in subviral-particle biogenesis. J Virol **87:**1491-1496.
27. **Eble BE, Lingappa VR, Ganem D.** 1990. The N-terminal (pre-S2) domain of a hepatitis B virus surface glycoprotein is translocated across membranes by downstream signal sequences. J Virol **64:**1414-1419.
28. **Lambert C, Thome N, Kluck CJ, Prange R.** 2004. Functional incorporation of green fluorescent protein into hepatitis B virus envelope particles. Virology **330:**158-167.
29. **Costantini LM, Subach OM, Jaureguiberry-bravo M, Verkhusha VV, Snapp EL.** 2013. Cysteineless non-glycosylated monomeric blue fluorescent protein, secBFP2, for studies in the eukaryotic secretory pathway. Biochem Biophys Res Commun **430:**1114-1119.
30. **Rocks O, Gerauer M, Vartak N, Koch S, Huang ZP, Pechlivanis M, Kuhlmann J, Brunsveld L, Chandra A, Ellinger B, Waldmann H, Bastiaens PI.** 2010. The palmitoylation machinery is a spatially organizing system for peripheral membrane proteins. Cell **141:**458-471.
31. **Mangold CM, Streeck RE.** 1993. Mutational analysis of the cysteine residues in the hepatitis B virus small envelope protein. J Virol **67:**4588-4597.
32. **da Silva DV, Nordholm J, Madjo U, Pfeiffer A, Daniels R.** 2013. Assembly of subtype 1 influenza neuraminidase is driven by both the transmembrane and head domains. J Biol Chem **288:**644-653.
33. **Prange R, Streeck RE.** 1995. Novel transmembrane topology of the hepatitis B virus envelope proteins. EMBO J **14:**247-256.
34. **Ostapchuk P, Hearing P, Ganem D.** 1994. A dramatic shift in the transmembrane topology of a viral envelope glycoprotein accompanies hepatitis B viral morphogenesis. EMBO J **13:**1048-1057.
35. **Bruss V, Ganem D.** 1991. Mutational analysis of hepatitis B surface antigen particle assembly and secretion. J Virol **65:**3813-3820.

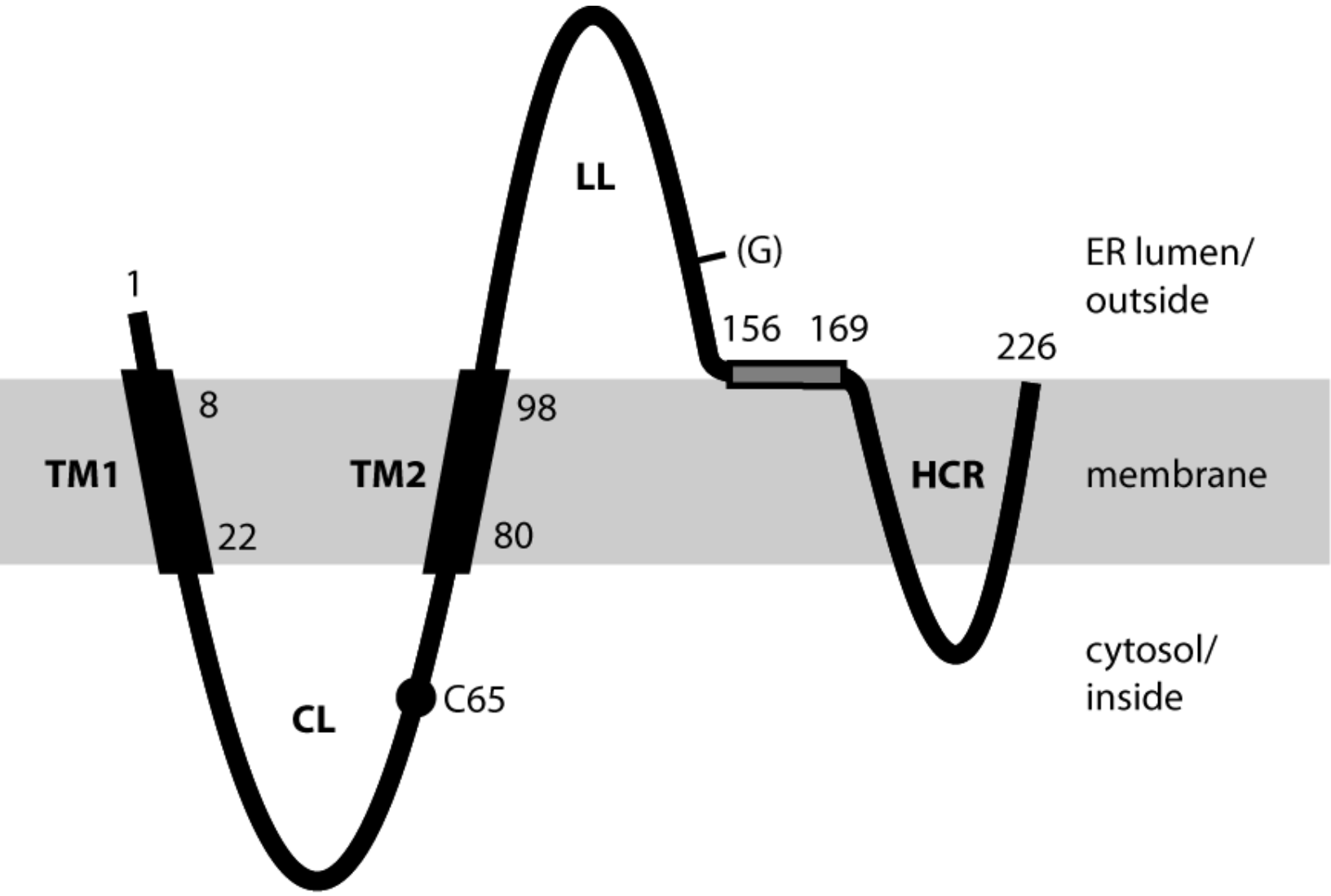

Suffner et al. Fig. 1

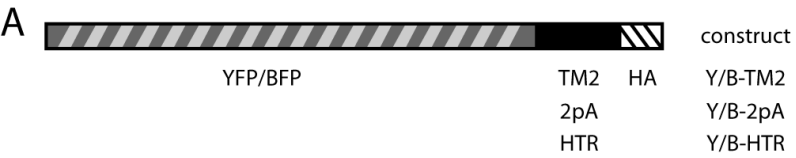

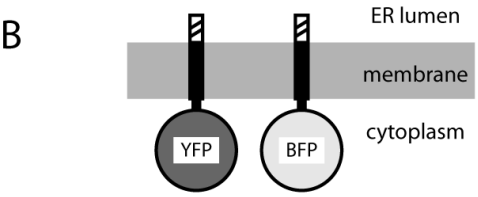

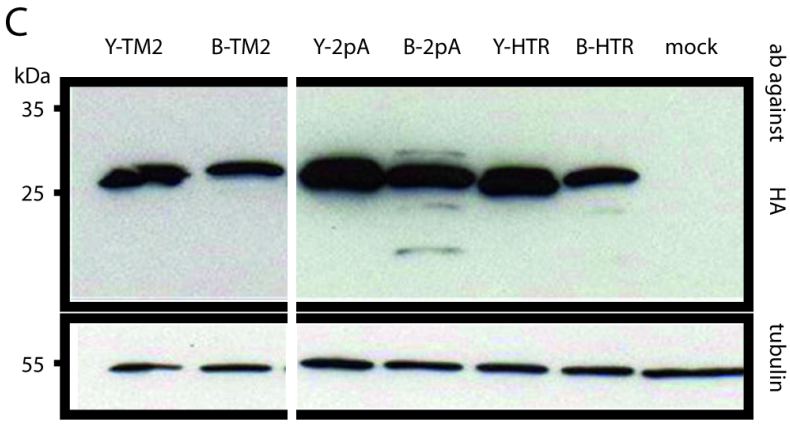

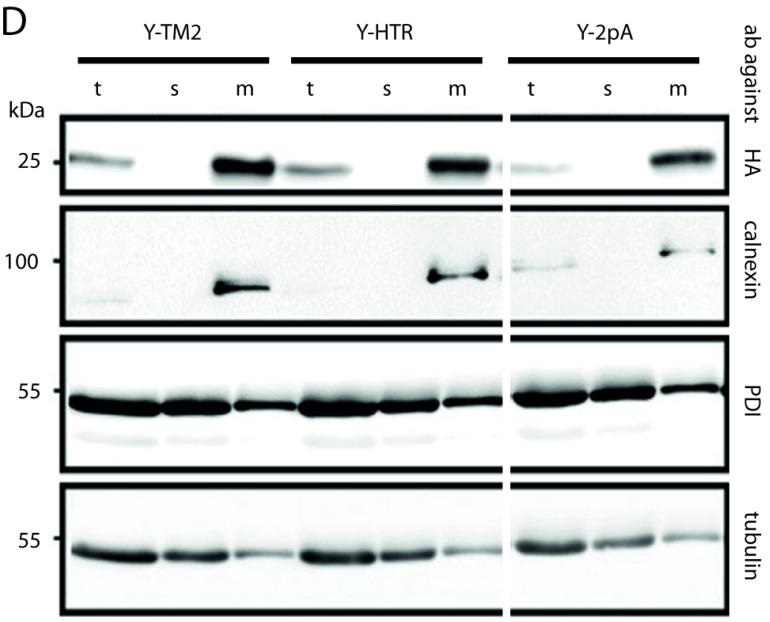

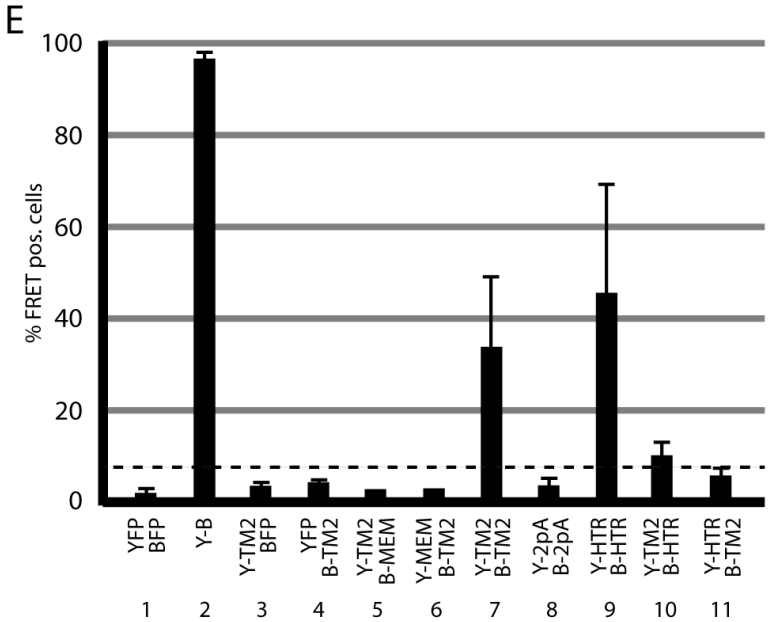

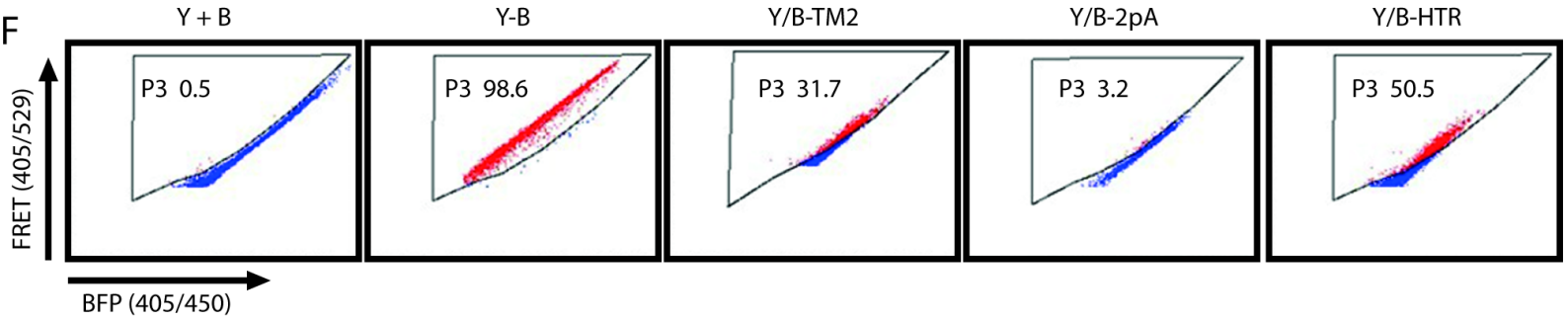

Suffner et al. Fig. 2

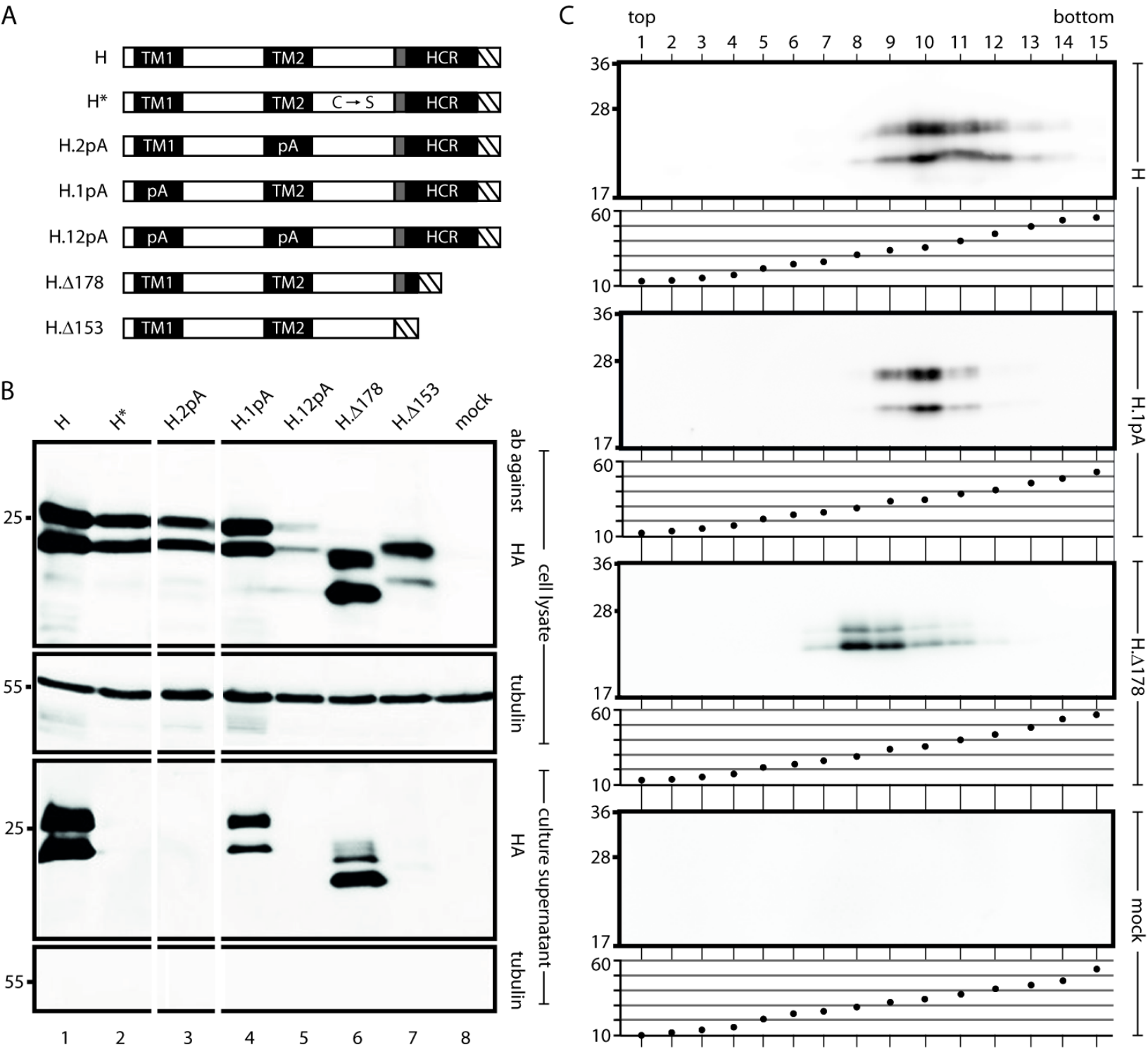

Suffner et al. Fig. 3

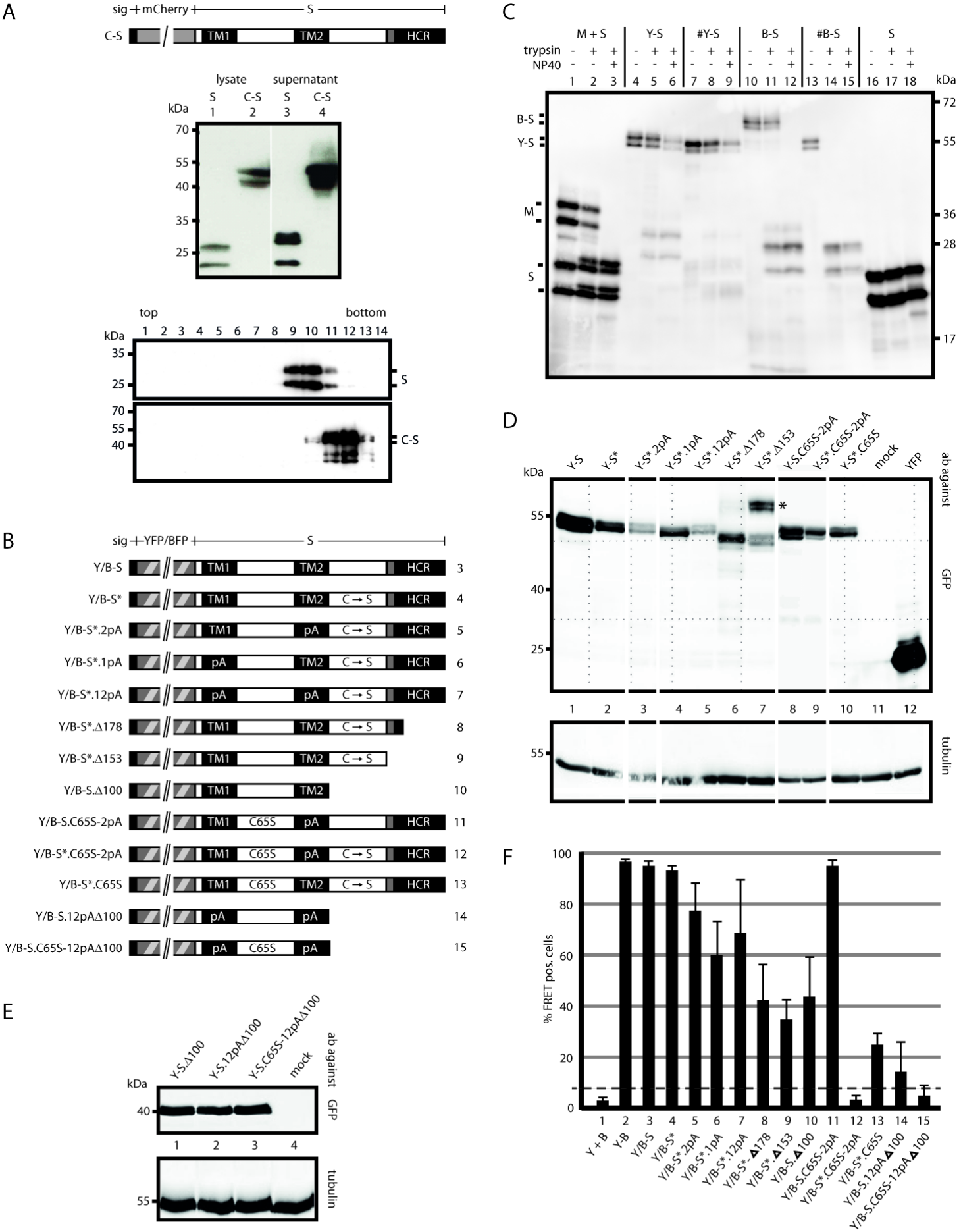

Suffner et al. Fig. 4A-F

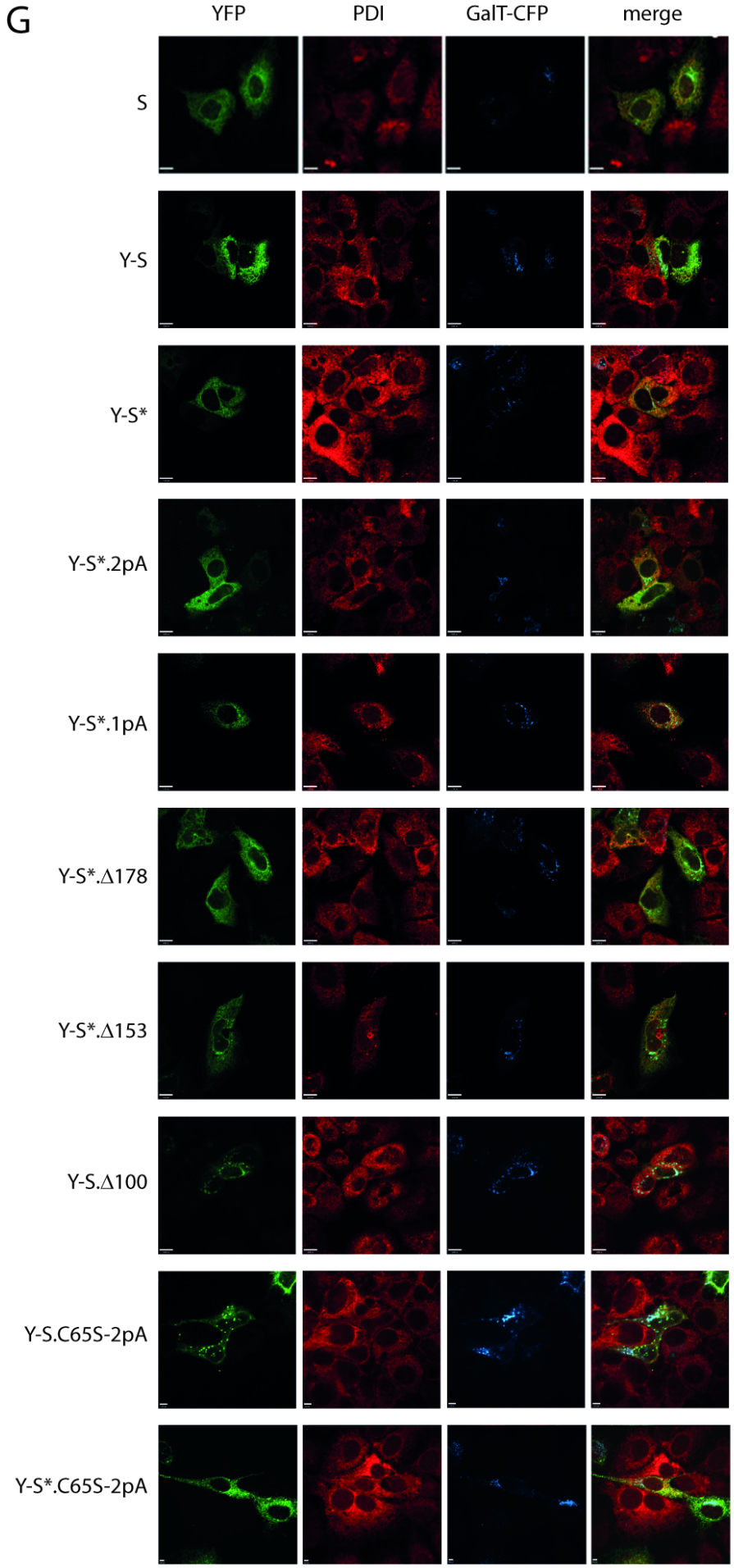

Suffner et al. Fig. 4G

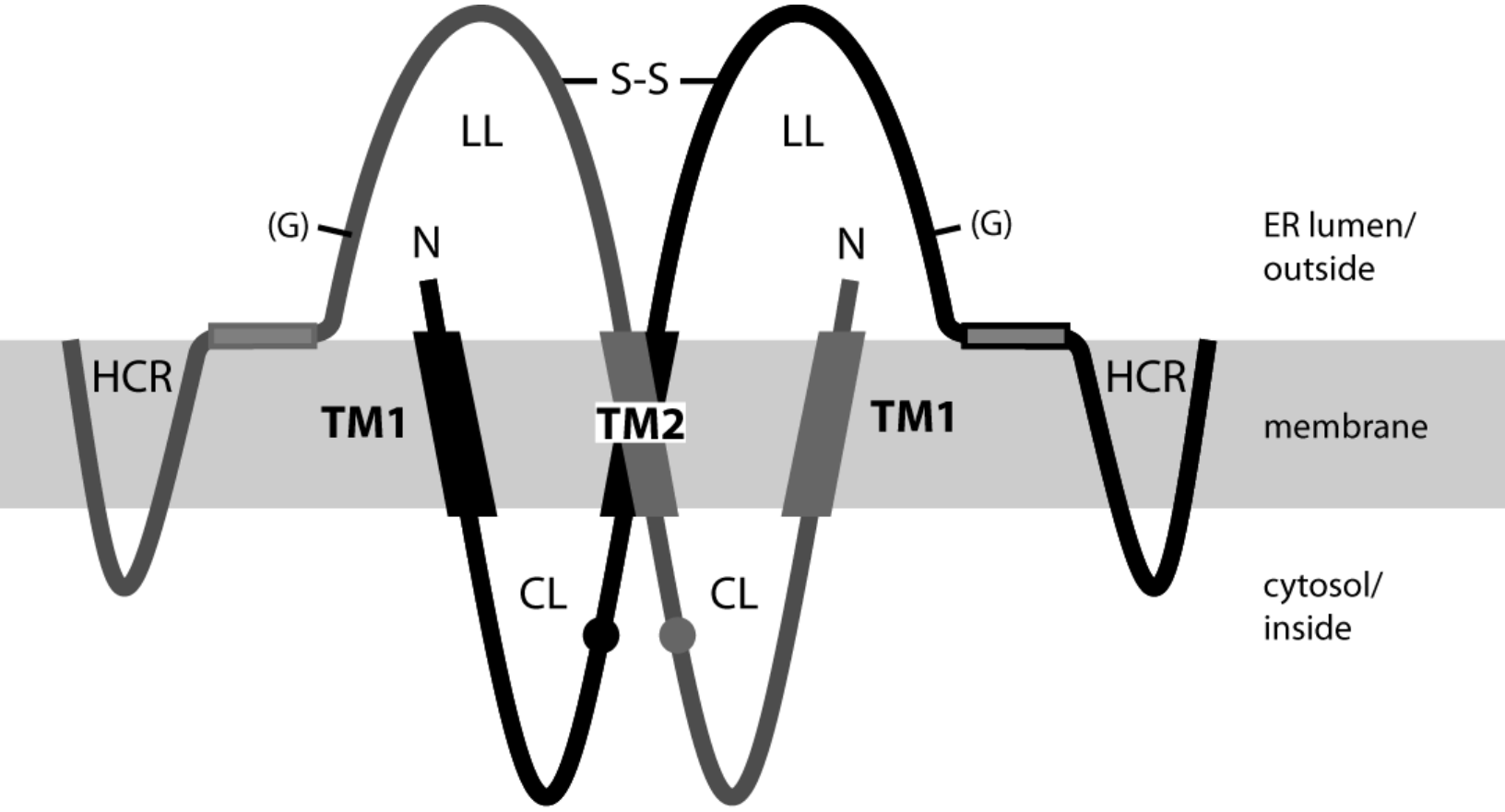

Suffner et al. Fig. 5